Supplementary Information

Can room temperature data for tunneling molecular junctions be analyzed within a theoretical framework assuming zero temperature?

Ioan Bâldea [a*]

Keywords: molecular electronics, nanojunctions, single level model, thermal effects

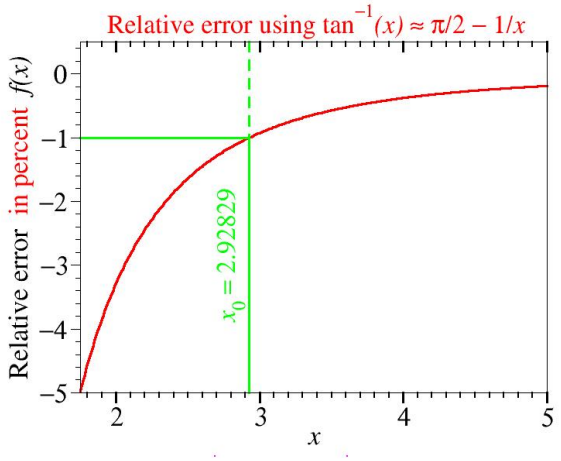

Fig. S1 Function $f(x) \equiv 100\left[(\pi/2 - 1/x)/\tan^{-1} x - 1\right]$ visualizing that the relative error in percent implied by using eqn (8a) is negligible.

[a] *Theoretical Chemistry, Heidelberg University, Im Neuenheimer Feld 229, D-69120 Heidelberg, Germany*
* E-mail: ioan.baldea@pci.uni-heidelberg.de

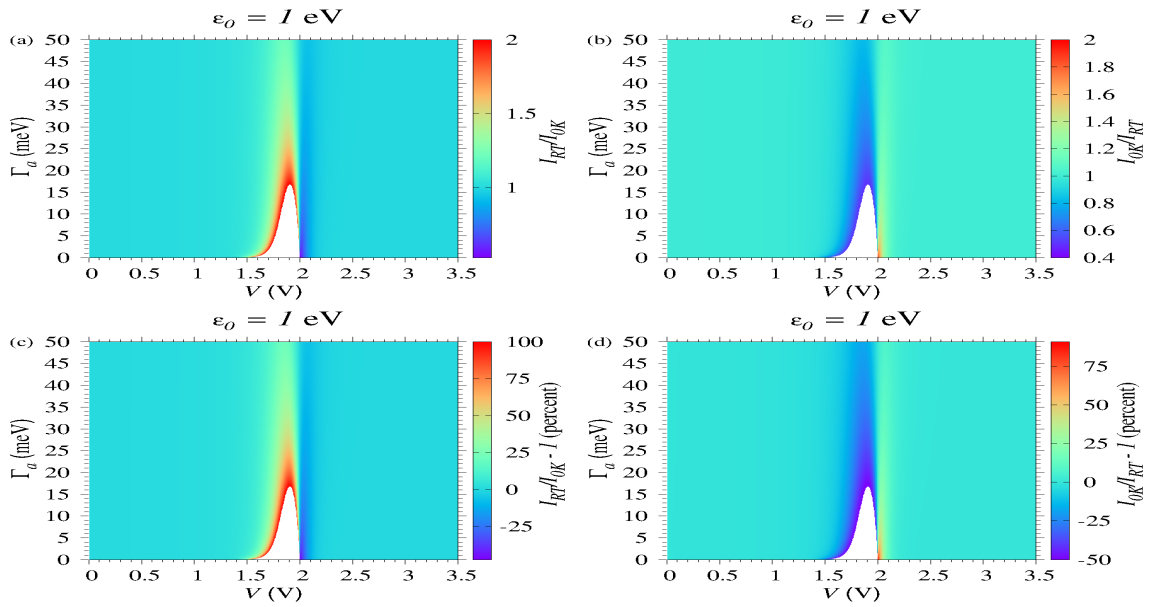

Fig. S2 Basically, the information presented in this figure on the deviations of the current I_{0K} computed at zero temperature using eqn (3) from the room temperature I_{RT} computed via eqn (1) is the same as that of Fig. 1a and b. We prefer the latter manner of presentation because we find it is easier to understand.

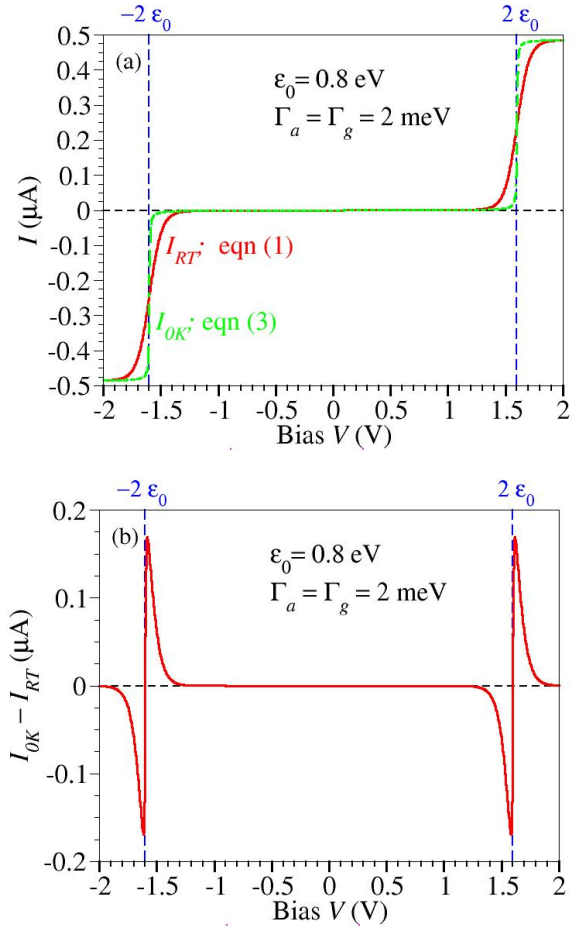

Fig. S3 (a) *I-V* curves computed using eqn (1) and eqn (3) illustrating that the thermal effect (b) enhances the current below resonance ($|I_{RT}| > |I_{0K}|$ for $|eV| < 2|\varepsilon_0|$) while reducing it above resonance ($|I_{RT}| < |I_{0K}|$ for $|eV| > 2|\varepsilon_0|$).

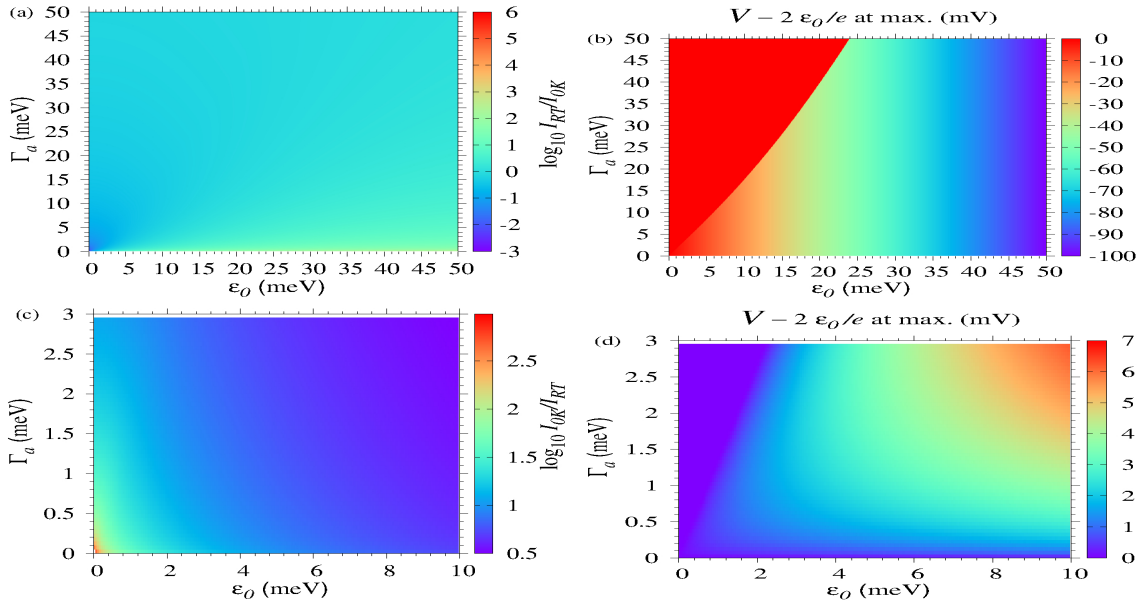

Fig. S4 Results at very small values of the MO offset ε_0 showing an opposite behavior to that at (reasonably) large ε_0. Panel (a) depicts situations below resonance wherein $I_{RT} < I_{0K}$. Likewise, panel c shows situations above resonance wherein $I_{0K} < I_{RT}$. The values of panel a (panel c) were computed at the biases V_m that maximize the ratio I_{RT}/I_{0K} (I_0/I_{RT}). The corresponding differences from resonance $V_m - 2\varepsilon_0/e$ are presented in panels b and d, respectively.

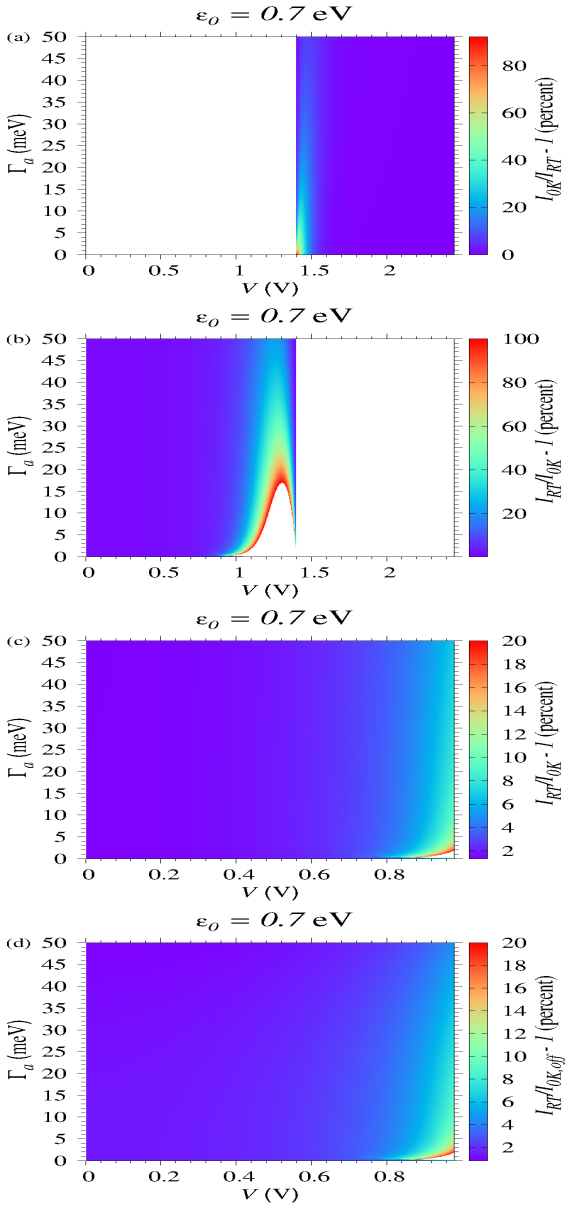

Fig. S5 The colored regions in the plane (V, Γ_a) depict situations where, at the fixed value of the MO energy offset indicated ($\varepsilon_0 = 0.7$ eV), the current I_{0K} computed at $T = 0$ using eqn (3) is larger ($|eV| > 2|\varepsilon_0|$, panel a) or smaller ($|eV| < 2|\varepsilon_0|$, panel b) than the exact current I_{RT} computed from eqn (1) at room temperature ($T = 298.15$ K). For parameter values compatible with eqn (10) and (11), the current $I_{0K,off}$ computed using eqn (9) is very accurate (panel d); it is as accurate as I_{0K} (panel c). Relative deviations (shown only when not exceeding 100%) are indicated in the color box. To facilitate comparison between $I_{0K,off}$ and I_{0K}, abscissas in panel c depicting I_{0K} are restricted to those in panel d. Notice that the z-range in panels (c) and (d) is different from panel b.

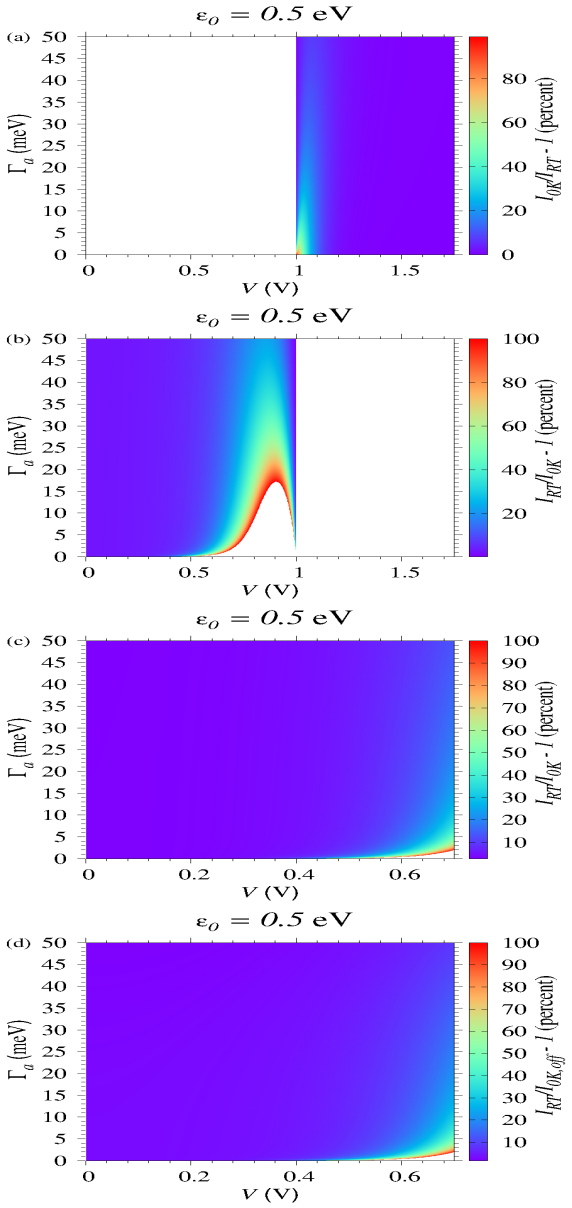

Fig. S6 The colored regions in the plane (V, Γ_a) depict situations where, at the fixed value of the MO energy offset indicated ($\varepsilon_0 = 0.5$ eV), the current I_{0K} computed at $T = 0$ using eqn (3) is larger ($|eV| > 2|\varepsilon_0|$, panel a) or smaller ($|eV| < 2|\varepsilon_0|$, panel b) than the exact current I_{RT} computed from eqn (1) at room temperature ($T = 298.15$ K). For parameter values compatible with eqn (10) and (11), the current $I_{0K,off}$ computed using eqn (9) is very accurate (panel d); it is as accurate as I_{0K} (panel c). Relative deviations (shown only when not exceeding 100%) are indicated in the color box. To facilitate comparison between $I_{0K,off}$ and I_{0K}, abscissas in panel c depicting I_{0K} are restricted to those in panel d. Notice that the z-range in panels (c) and (d) is different from panel b.

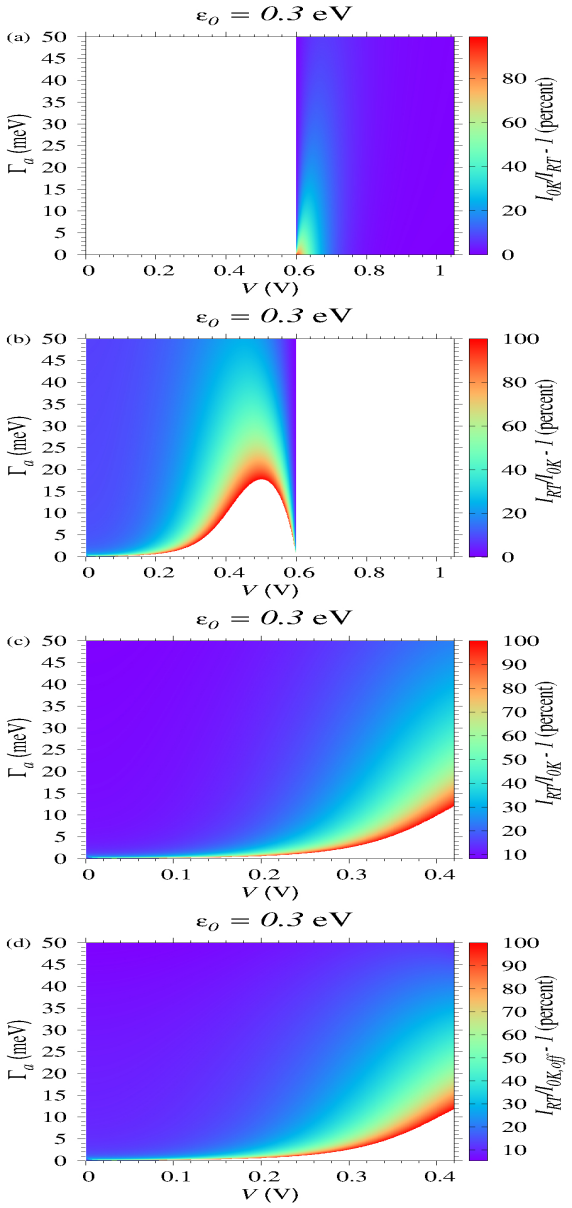

Fig. S7 The colored regions in the plane (V, Γ_a) depict situations where, at the fixed value of the MO energy offset indicated ($\varepsilon_0 = 0.3$ eV), the current I_{0K} computed at $T = 0$ using eqn (3) is larger ($|eV| > 2|\varepsilon_0|$, panel a) or smaller ($|eV| < 2|\varepsilon_0|$, panel b) than the exact current I_{RT} computed from eqn (1) at room temperature ($T = 298.15$ K). For parameter values compatible with eqn (10) and (11), the current $I_{0K,off}$ computed using eqn (9) (panel d) is as accurate as I_{0K} (panel c). Relative deviations (shown only when not exceeding 100%) are indicated in the color box. To facilitate comparison between $I_{0K,off}$ and I_{0K}, abscissas in panel c depicting I_{0K} are restricted to those in panel d. Notice that the z-range in panels (c) and (d) is different from panel b.

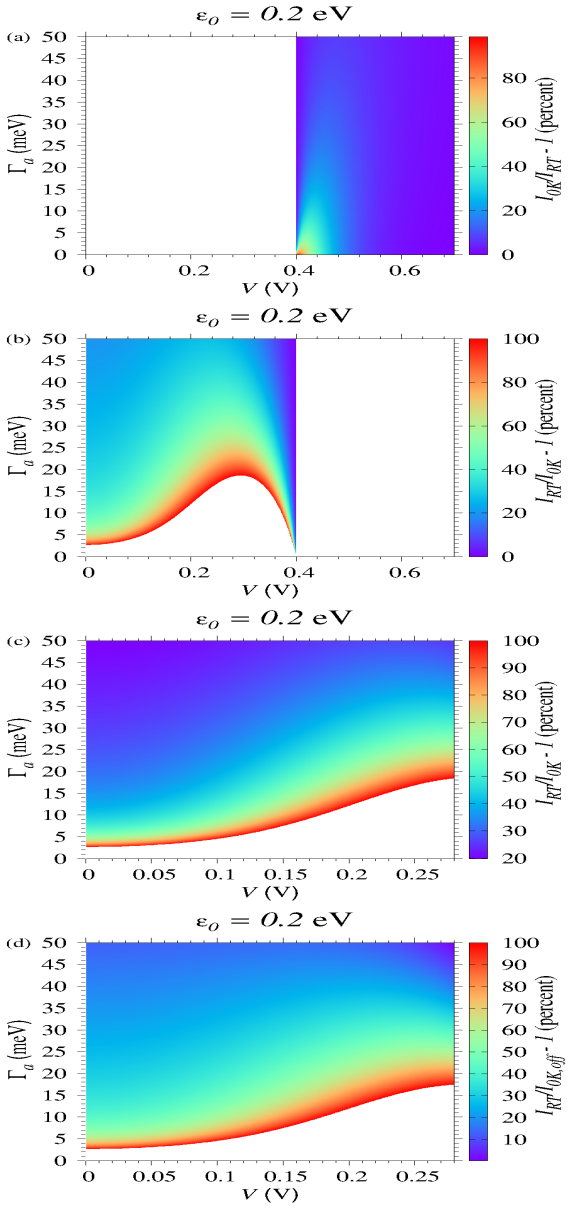

Fig. S8 The colored regions in the plane (V, Γ_a) depict situations where, at the fixed value of the MO energy offset indicated ($\varepsilon_0 = 0.2$ eV), the current I_{0K} computed at $T = 0$ using eqn (3) is larger ($|eV| > 2|\varepsilon_0|$, panel a) or smaller ($|eV| < 2|\varepsilon_0|$, panel b) than the exact current I_{RT} computed from eqn (1) at room temperature ($T = 298.15$ K). For parameter values compatible with eqn (10) and (11), the current $I_{0K,off}$ computed using eqn (9) (panel d) is as accurate as I_{0K} (panel c). Relative deviations (shown only when not exceeding 100%) are indicated in the color box. To facilitate comparison between $I_{0K,off}$ and I_{0K}, abscissas in panel c depicting I_{0K} are restricted to those in panel d. Notice that the z-range in panels (c) and (d) is different from panel b.

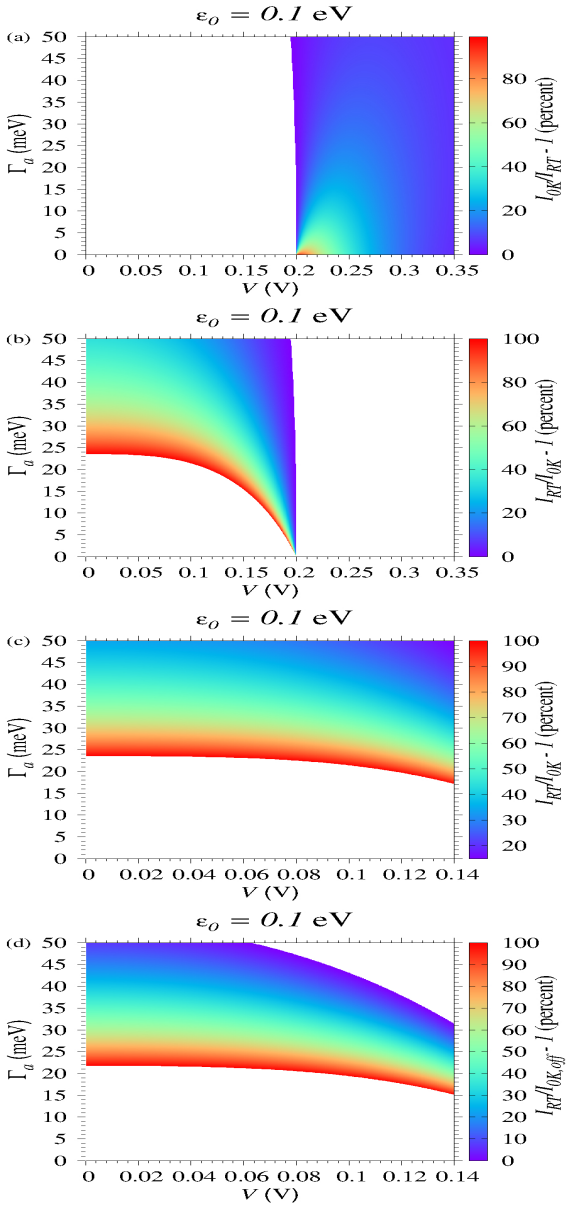

Fig. S9 The colored regions in the plane (V, Γ_a) depict situations where, at the fixed value of the MO energy offset indicated ($\varepsilon_0 = 0.1$ eV), the current I_{0K} computed at $T = 0$ using eqn (3) is larger ($|eV| > 2|\varepsilon_0|$, panel a) or smaller ($|eV| < 2|\varepsilon_0|$, panel b) than the exact current I_{RT} computed from eqn (1) at room temperature ($T = 298.15$ K). For situations violating eqn (11), the current $I_{0K,off}$ computed using eqn (9) (panel d) stronger departs from I_{RT} than I_{0K} (panel d). Relative deviations (shown only when not exceeding 100%) are indicated in the color box. To facilitate comparison between $I_{0K,off}$ and I_{0K}, abscissas in panel c depicting I_{0K} are restricted to those in panel d. Notice that the z-range in panels (c) and (d) is different from panel b.

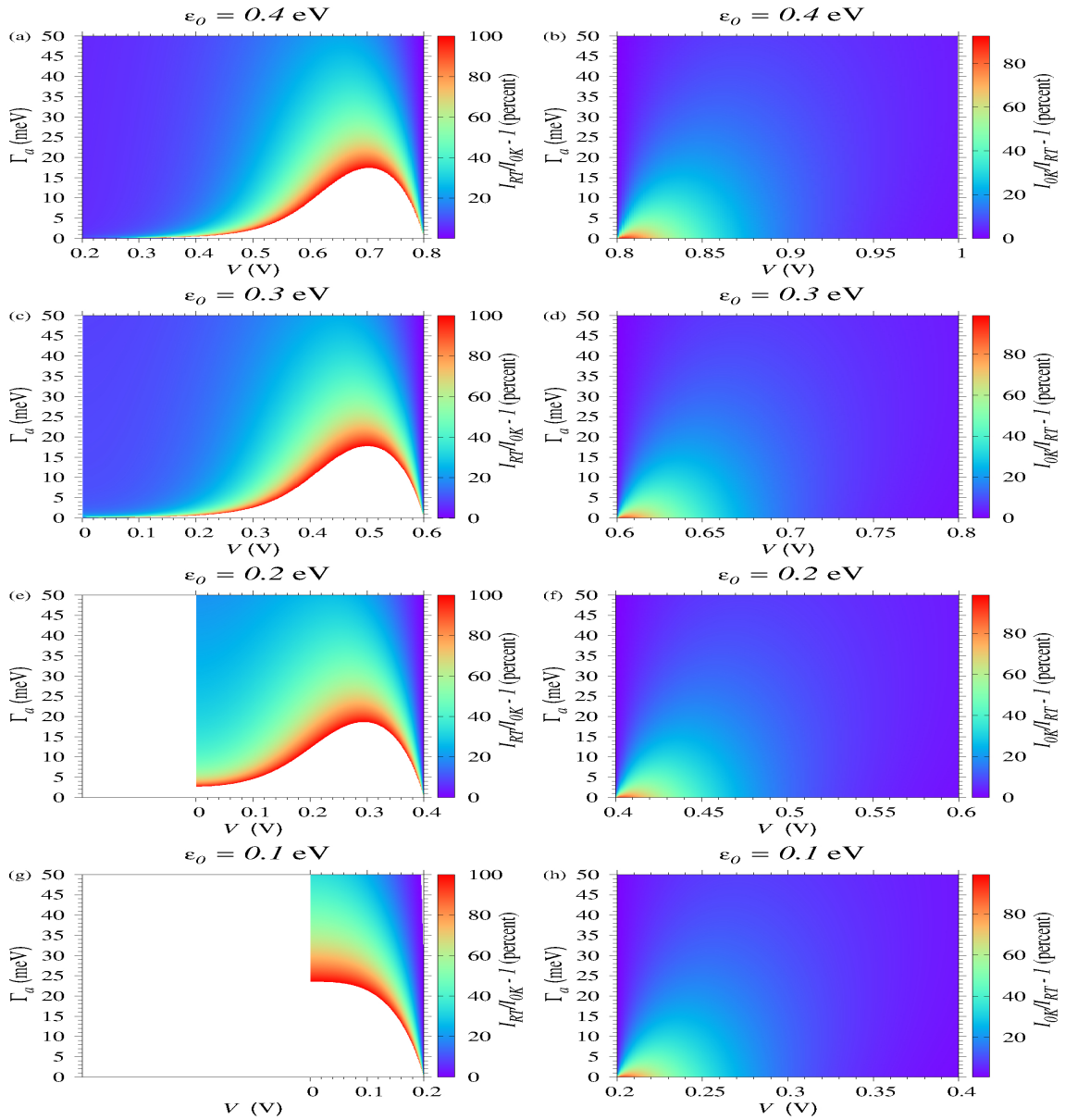

Fig. S10 Results for lower biases illustrating the current enhancement below resonance ($|eV| < 2\,|\varepsilon_0|$, left panels) and current reduction above resonance ($|eV| > 2\,|\varepsilon_0|$, right panels). As ε_0 decreases (downwards), the white (empty) region (wherein the relative deviations exceed 100%) in the left panels extends upwards to larger Γ_a and comprises a broader bias range. Notice that all rightmost (leftmost) positions of the left (right) panels are aligned to resonance.

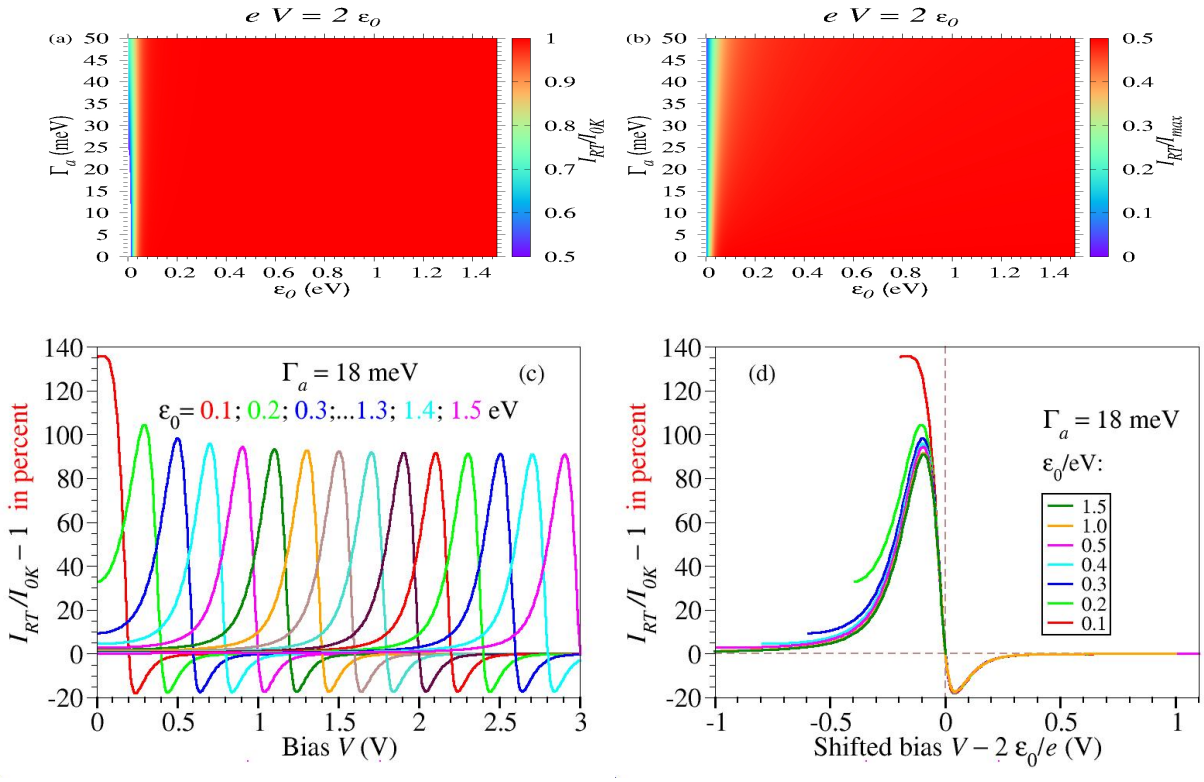

Fig. S11 (a,b) Strictly on resonance, the temperature impact on the current is negligible. (c,d) Except for small values of the MO energy offset ε_0, the thermal enhancement of the current occurs around resonance and is quite insensitive to ε_0.

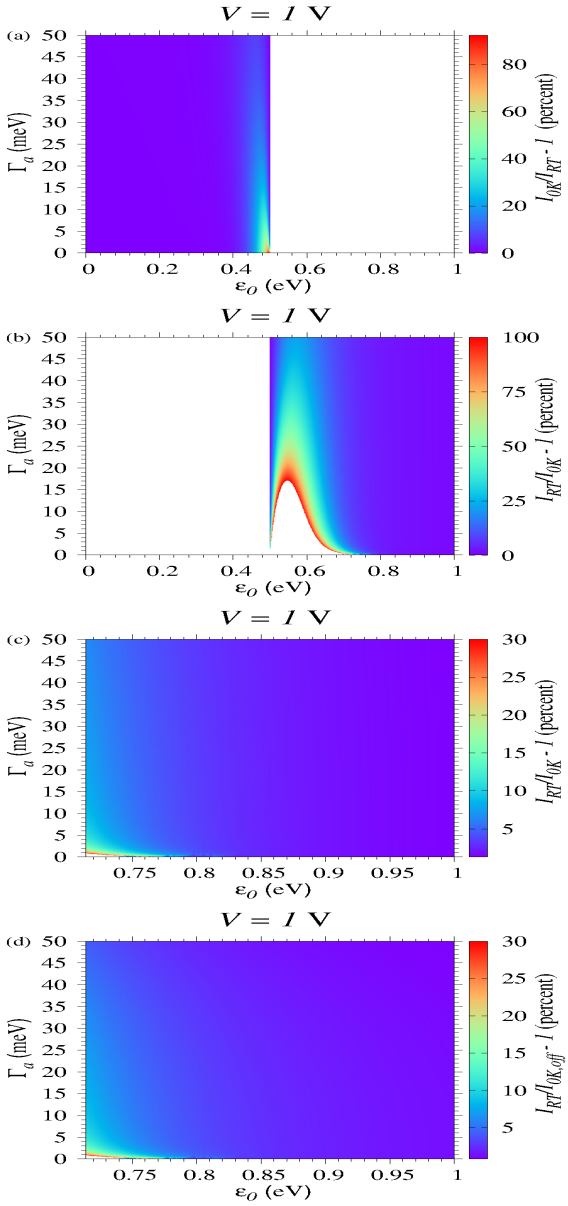

Fig. S12 The colored regions in the plane $(\varepsilon_0, \Gamma_a)$ depict situations where, at the fixed bias indicated ($V = 1$ V), the current I_{0K} computed at $T = 0$ using eqn (3) is larger ($|eV| > 2|\varepsilon_0|$, panel a) or smaller ($|eV| < 2|\varepsilon_0|$, panel b) than the exact current I_{RT} computed from eqn (1) at room temperature ($T = 298.15$ K). For parameter values compatible with eqn (10) and (11), the current $I_{0K,off}$ computed using eqn (9) is very accurate (panel d); it is as accurate as I_{0K} (panel c). Relative deviations (shown only when not exceeding 100%) are indicated in the color box. To facilitate comparison between $I_{0K,off}$ and I_{0K}, abscissas in panel c depicting I_{0K} are restricted to those in panel d. Notice that the z-range in panels (c) and (d) is different from panel b.

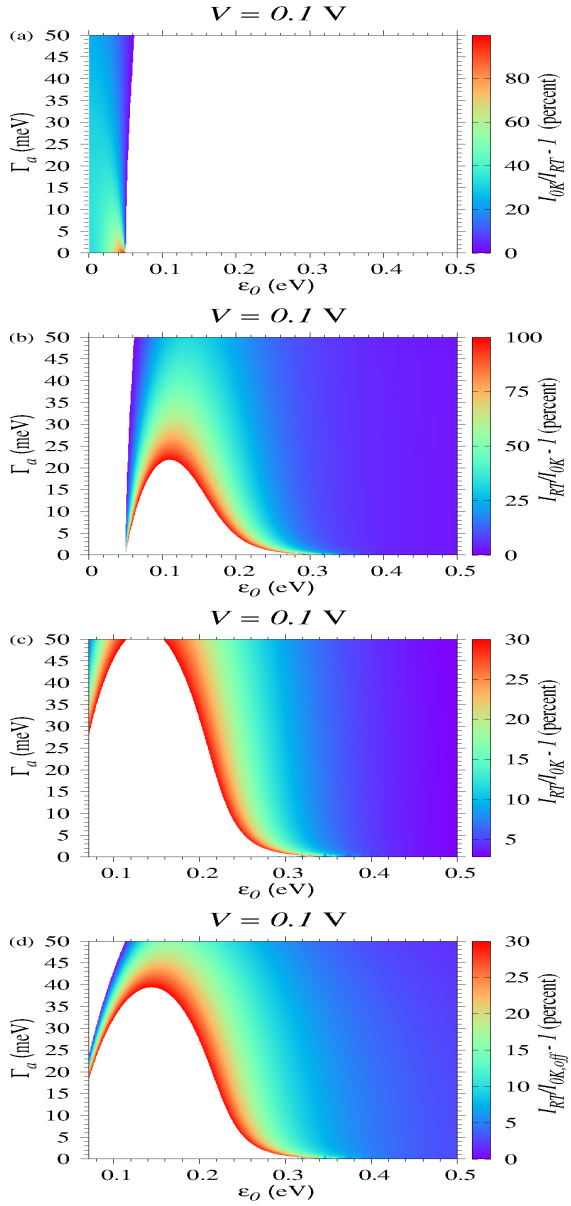

Fig. S13 The colored regions in the plane $(\varepsilon_0, \Gamma_a)$ depict situations where, at the fixed bias indicated ($V = 0.1$ V), the current I_{0K} computed at $T = 0$ using eqn (3) is larger ($|eV| > 2|\varepsilon_0|$, panel a) or smaller ($|eV| < 2|\varepsilon_0|$, panel b) than the exact current I_{RT} computed from eqn (1) at room temperature ($T = 298.15$ K). The fact that in this case, paradoxically, the current $I_{0K,off}$ computed using eqn (9) (panel d) is closer to I_{RT} than I_{0K} (panel c) is an error compensation effect. Relative deviations (shown only when not exceeding 100%) are indicated in the color box. To facilitate comparison between $I_{0K,off}$ and I_{0K}, abscissas in panel c depicting I_{0K} are restricted to those in panel d. Notice that the z-range in panels (c) and (d) is different from panel b.

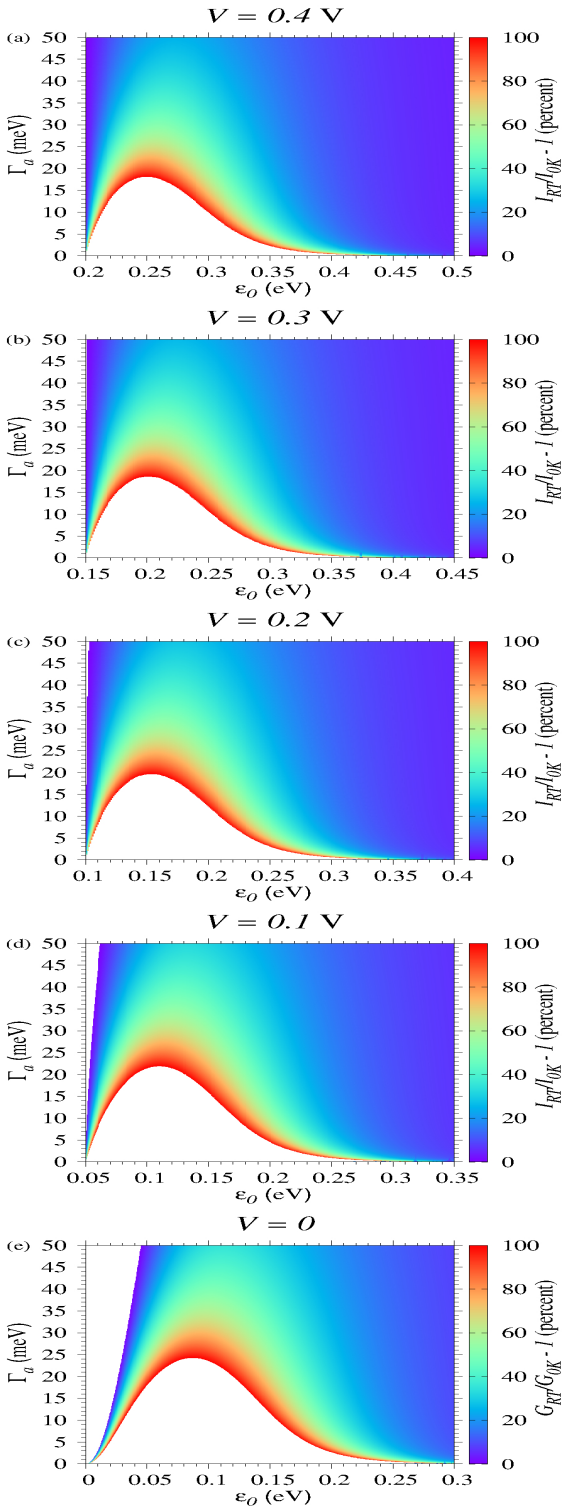

Fig. S14 Results illustrating the current enhancement below resonance ($|eV| < 2|\varepsilon_0|$) at lower biases. As the bias decreases (downwards), the white (empty) region (wherein the relative deviations exceed 100%) extends upwards to larger Γ_a and comprises a broader ε_0-range. Notice that the leftmost positions of all panels are aligned to resonance.

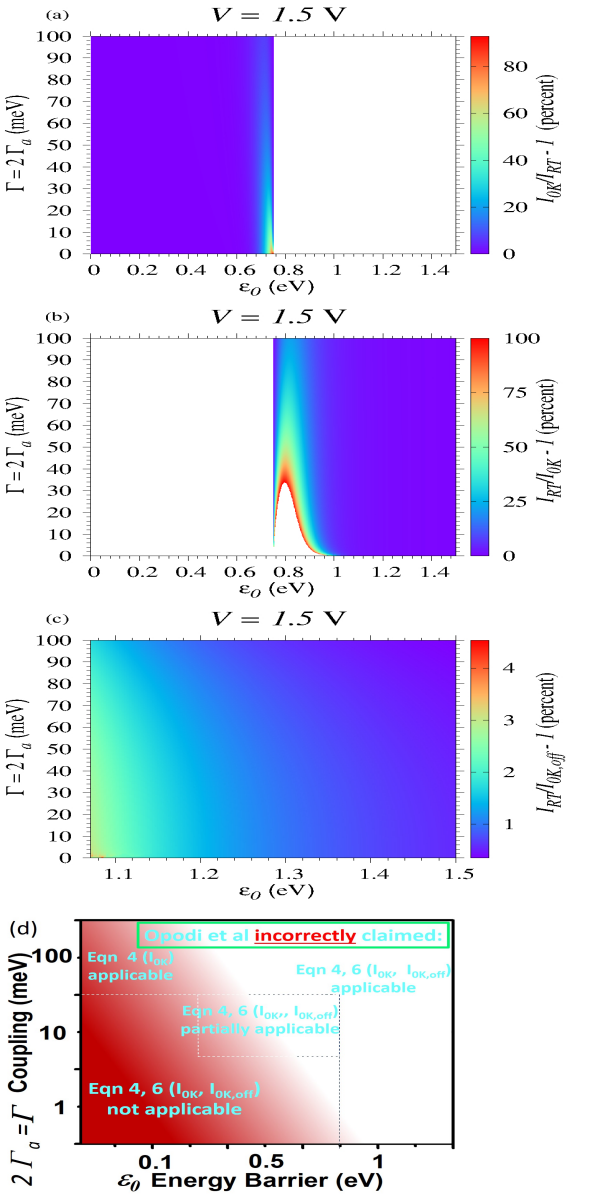

Fig. S15 Relative deviations in percent of the currents I_{0K} (panel a and b) and $I_{0K,off}$ (panel c) computed via eqn (3) and (9) assuming zero temperature from the exact current I_{RT} computed at room temperature. Comparison with panel d (adapted from Opodi et al, Phys. Chem. Chem. Phys. 2022, 24, 11958 and ref. 26) demonstrates that Fig. 5 of Opodi et al is a factual error. Notice that, in order to facilitate comparison with the paper by Opodi et al, the electronic coupling $\Gamma = 2\Gamma_a$ in panel d is different from Fig. 4.

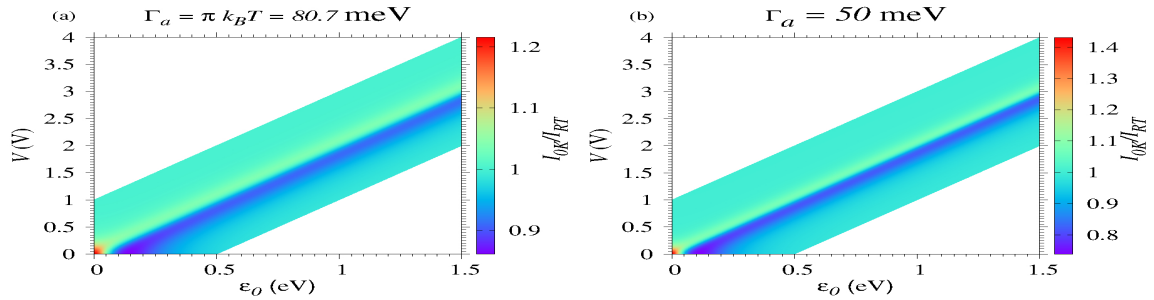

Fig. S16 Panel b visualizes the weak impact of the (room) temperature on the current at the highest value $\Gamma_a = 50$ meV chosen in most diagrams, which is even smaller than the value $\Gamma_a = \pi k_B T_{RT} = 80.7$ meV (panel a) where a weak temperature effect can be expected in view of eqn (13a).

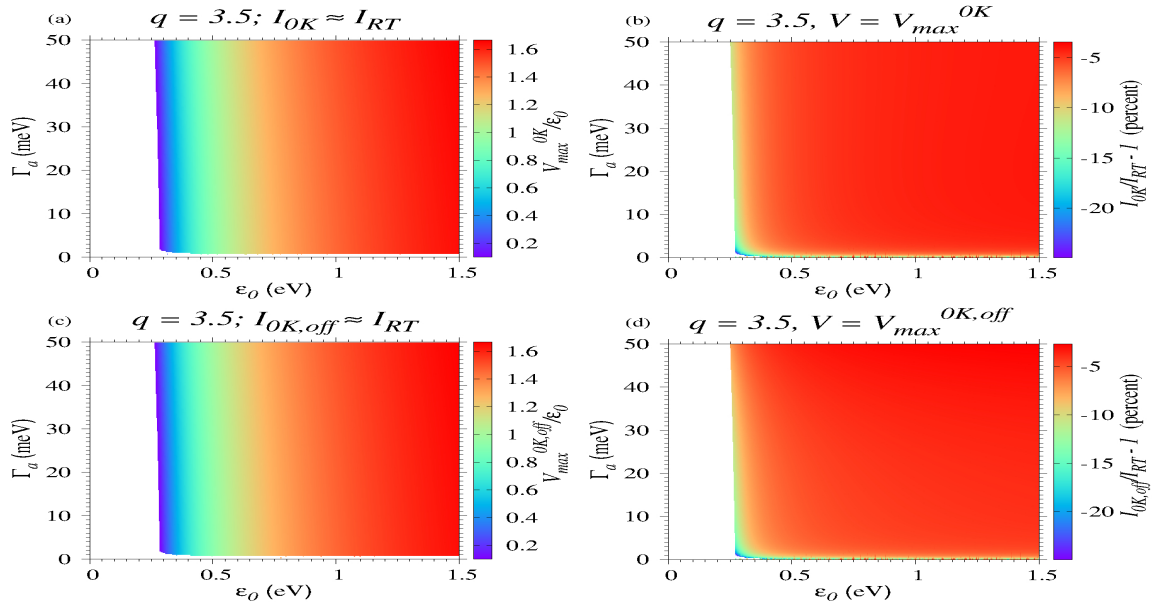

Fig. S17 Similar to Fig. 9 but setting $q = 3.5$ in eqn (13b).

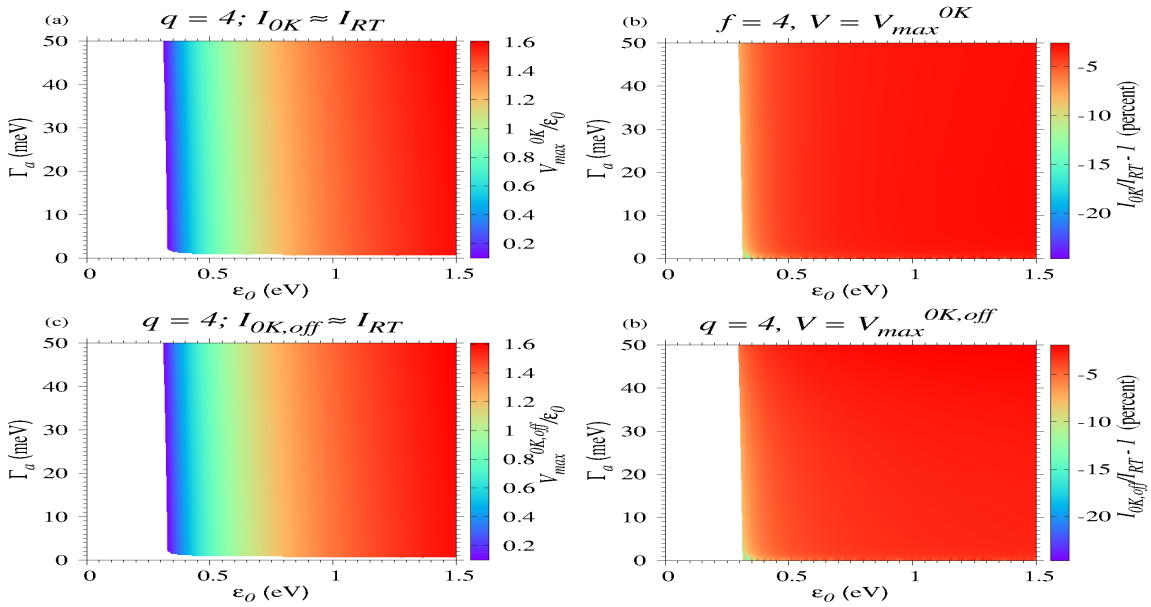

Fig. S18 Similar to Fig. 9 but setting $q = 4$ in eqn (13b).

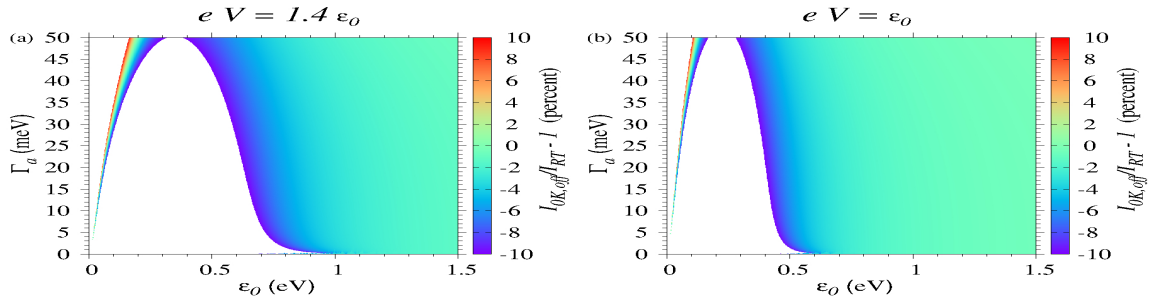

Fig. S19 This figure illustrates how restriction to the narrower bias range $|eV| < |\varepsilon_0|$ (panel b) can render data fitting using $I_{0K,off}$ (eqn (9)) applicable for junctions having, e.g., $\varepsilon_0 \simeq 0.5$ eV, a fact impossible when using the broader bias range $|eV| < 1.4\ |\varepsilon_0|$ (panel a).